Quarter-Mode Cavity Filters in Substrate Integrated Waveguide Technology

Stefano Moscato, *Student Member, IEEE*, Cristiano Tomassoni, *Member, IEEE*, Maurizio Bozzi, *Senior Member, IEEE*, Luca Perregrini, *Fellow, IEEE*

***Abstract*—This paper presents a systematic investigation of quarter-mode filters in substrate integrated waveguide (SIW) technology. This class of filters is particularly convenient because it combines the features of SIW structures with the improvement of a size reduction. After a thorough analysis of the quarter-mode SIW cavity, the paper presents different coupling mechanisms and feeding techniques for the design of quarter-mode SIW filters: side coupling and corner coupling are considered, highlighting advantages and disadvantages of the two techniques. Novel filter topologies are introduced, with the design and experimental verification of simple filters and their extension to higher-order filter structures. Techniques to introduce transmission zeros are described and demonstrated. Moreover, the combination of quarter-mode SIW cavities and coplanar-waveguide resonators leads to increasing the filter order higher-order and allows for the implementation of quasi-elliptic filters.**

***Index Terms*—Filter, quarter-mode cavity, resonant cavity, substrate integrated waveguide (SIW).**

I. Introduction

The recent development of a large variety of applications in the microwave and mm-wave frequency range poses several technological requirements for the next generation of wireless systems. These emerging applications demand for a new class of microwave circuits, which are cost-effective, compact, easy to fabricate, and suitable for system integration.

Among the available technologies for the implementation and integration of microwave components, the substrate integrated waveguide (SIW) [1] appears to be one of the best candidates to meet all these technological requirements. The SIW is a waveguide-like structure integrated in planar form [2], which preserve the best features of the classical rectangular waveguide, including low losses, practically complete electromagnetic shielding, and self-packaging. The SIW can be manufactured in a reliable and cost-effective way by adopting standard printed-circuit board technology, typically used for microstrip line components.

One of the few drawbacks of SIW technology is related to the footprint of SIW components, which is generally larger than in the microstrip line counterparts. In fact, the width of SIW structures depends on the operation frequency, which usually falls in the single-mode frequency band of the waveguide. Several solutions have been proposed to reduce the footprint of SIW structures, including the substrate integrated folded waveguide [3] and the half-mode substrate integrated waveguide [4]. These two topologies allow for reducing of a factor two the width of the SIW.

In particular, SIW filters suffer from the same shortcoming: for instance, in SIW cavity filters the size of each cavity is approximately half wavelength times half wavelength [5]. Also in the case of SIW filters, several methods have been proposed to reduce the footprint, based on folded topologies [6,7] and half-mode configurations [8,9]. Moreover, quarter-mode cavities are receiving increasing attention for the design of SIW filters [10–19]. Quarter-mode SIW filters were first proposed and demonstrated in [10] by using a geometric configuration allowing for filters up to the 4th order. A two-pole band-pass filter with transmission zeros due to source-load cross-coupling was introduced in [11]. Different quarter-mode SIW filter topologies were subsequently presented in [13,15,16]. Reconfigurable filters were introduced in [12,19], and quarter-mode SIW filters combined with defected ground structures were proposed in [14,17,18].

This paper presents a systematic investigation of quarter-mode SIW filters, to enable their full exploitation in the design of single-layer band-pass filters with high selectivity and small footprint. New configurations and topologies are here proposed, some of them allowing for an arbitrary filter order. Sec. II reports a thorough analysis of the basic characteristics of quarter-mode SIW cavities and the comparison with standard SIW cavities. Subsequently, the different coupling mechanisms and feeding techniques are investigated in details, to show the possibility of weak or strong coupling between the SIW cavities and, consequently, the ability to design filters with narrow or large relative bandwidth: side coupling is presented in Sec. III, and corner coupling is illustrated in Sec. IV. The design of novel filter topologies with different complexity (e.g., various order, presence of transmission zeros) is presented in Sec. V. In all sections, the experimental verification of the most significant filters is reported.

II. The Quarter-Mode SIW Cavity

The quarter-mode SIW cavity is obtained by cutting the standard SIW cavity along the symmetry planes and removing the top metal wall and the metal vias of three quarters of the structure (Fig. 1). Consequently, only one quarter of the structure is retained and the size is reduced of 75% compared

Paper submitted Sept. 24, 2015; revised March 27, 2016; accepted May 29, 2016. This work was supported in part by the Italian Ministry of Education, University and Scientific Research under the project PRIN "GreTa" 2010WHY5PR.

S. Moscato, M. Bozzi, and L. Perregrini are with the University of Pavia, Department of Electrical, Computer and Biomedical Engineering, Pavia, Italy (e-mail: ste.moscato@gmail.com, maurizio.bozzi@unipv.it, luca.perregrini@unipv.it).

C. Tomassoni is with the University of Perugia, Department of Engineering, Perugia, Italy (e-mail: cristiano.tomassoni@diei.unipg.it).

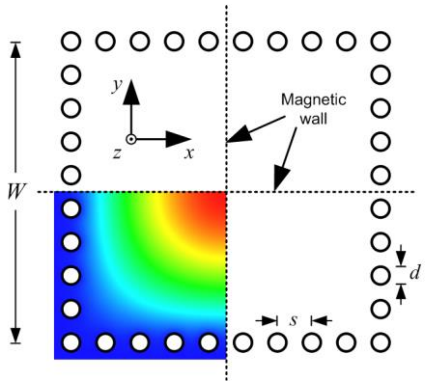

Fig. 1. Amplitude of the electric modal field of the fundamental TM_{110} mode of the SIW cavity, in the remaining quarter cavity obtained after cutting along the symmetry planes.

to the standard SIW cavity. Due to the low aspect ratio of the SIW, the open sides behave approximately as magnetic walls: therefore, the modes of the original cavity that satisfy the magnetic wall condition along the symmetry planes are unaffected, whereas the other modes are not supported by the quarter-mode SIW cavity.

More specifically, the quarter-mode SIW cavity only supports TM-to-*z* modes and, due to the similarity with the standard rectangular cavity with solid metal walls, the supported modes are denoted as TM_{mnp}, where the modal indices *m*, *n*, and *p* refer to the *x*, *y*, and *z* axes, respectively (Fig. 1). As there is no field variation along the *z* direction [1], $p=0$ for all cavity modes. The fundamental mode of the quarter-mode SIW cavity is the TM_{110} mode, whose electric modal field is shown in Fig. 1. Due to the presence of the magnetic walls at the open sides, the higher order modes are TM_{mn0}, with odd values of *m* and *n*. The direct effect of this phenomenon is a larger frequency separation between the resonance frequency f_0 of the fundamental mode and the one of the second mode. In fact, in a square standard SIW cavity the second mode (TM_{120} or TM_{210}) resonates at $1.58f_0$, whereas in a square quarter-mode SIW cavity the second mode (TM_{130} or TM_{310}) resonates at $2.24f_0$. The frequency separation between the first and second mode with the quarter-mode SIW cavity shown in Fig. 1 is larger than the one achieved in [15] with a different segmentation of the SIW cavity.

The quality factors of the quarter-mode SIW cavity modes are related to dielectric and conductor loss (as in the standard SIW cavity), and to the additional loss due to radiation leakage (which is typically negligible in standard SIW cavities). For a quantitative comparison between standard and quarter-mode SIW cavities, a specific structure is investigated by a full-wave simulation based on the eigensolver of Ansys HFSS. The dimensions of the SIW cavity have been selected to have the fundamental TM_{110} mode resonance at approximately 4 GHz, considering a dielectric substrate with $\varepsilon_r=3.5$, $\tan\delta=0.0018$, and thickness $t=0.508$ mm. The resulting dimensions are $W=29.15$ mm, $d=1.5$ mm, and $s=2.65$ mm (Fig. 1). The different contributions to the total quality factor Q_{tot} of the fundamental mode of the two cavities have been computed separately by using Ansys HFSS: Tab. I reports the quality factor Q_d due to dielectric loss, Q_c due to conductor loss, and Q_{rad} due to radiation loss, together with the total quality factor Q_{tot}. The quality factor Q_d can be estimated by analogy with the standard rectangular cavity, as $Q_d=1/\tan\delta$ [20] resulting in this case $Q_d=556$. The quarter-mode SIW cavity exhibits a value Q_d slightly larger than the standard SIW cavity, due to the fringing fields in the air at the open

TABLE I COMPARISON OF QUALITY FACTORS OF STANDARD SIW CAVITY AND QUARTER-MODE SIW CAVITY.

	Standard SIW cavity	Quarter-mode SIW cavity
Q_d	556	587
Q_c	466	423
Q_{rad}	---	390
Q_{tot}	254	151

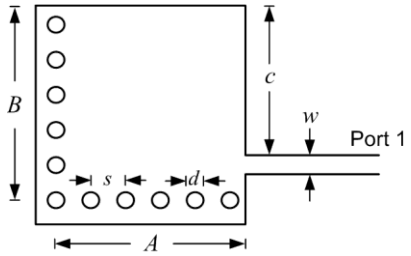

(*a*)

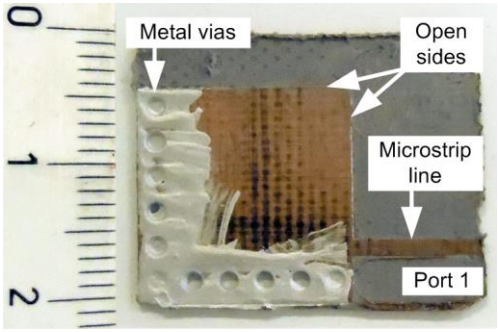

(*b*)

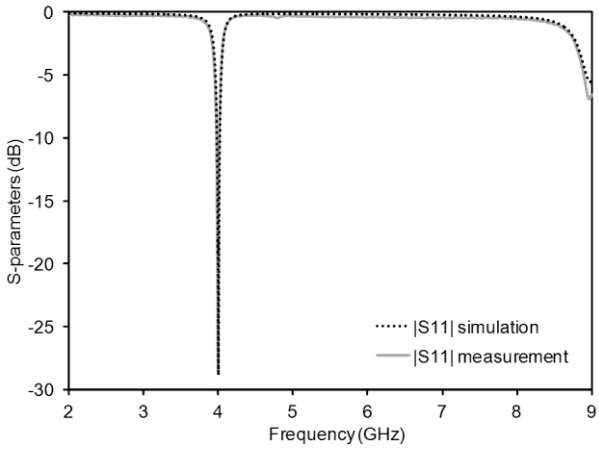

(*c*)

Fig. 2. Quarter mode SIW cavity (dimensions in mm: $A=B=14.6$, $c=11.6$, $s=2.65$, $d=1.5$, $w=1.2$): (*a*) drawing of the structure; (*b*) photograph of the prototype; (*c*) simulated and measured $|S_{11}|$ parameter.

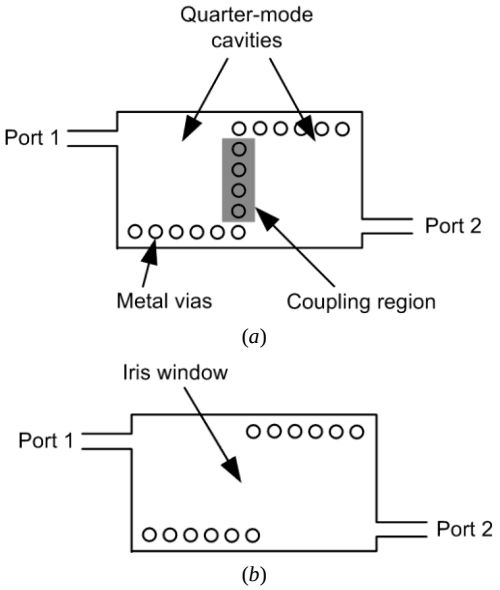

Fig. 3. Quarter-mode SIW filter with side coupling: (*a*) two separated quarter-mode SIW cavities (the dark gray area denotes the coupling region); (*b*) schematic of a two-cavity filter with side coupling.

sides. Also the quality factor Q_c can be estimated by analogy with the standard rectangular cavity [20], resulting in this case Q_c=466. The quality factor Q_c is slightly smaller in the quarter-mode cavity, due to extra loss of the current flowing near the sharp edge at the open sides. Differently from other compact cavities (e.g., ridge cavities), the contribution of conductor loss practically does not increase in the case of the quarter-mode SIW in spite of the significant size reduction. Furthermore, while the standard SIW cavity has negligible radiation loss, the quarter-mode cavity exhibits a loss due to radiation comparable to conductor loss ($Q_{rad} \approx Q_c$). Q_{rad} needs to be computed numerically, as nor specific formulas or analogy with the standard rectangular cavity are available.

To experimentally verify the performance of quarter-mode SIW cavities, a prototype has been designed and fabricated (Fig. 2). The dimensions are derived from the previous theoretical investigation and are reported in the caption of Fig. 2. The position of the 50 Ω microstrip feed line has been selected for optimal input matching: due to the field distribution, the impedance seen at the feed point is maximum at the open corner (*c*=0) and vanishes near the metal vias (*c*=*B*). A prototype has been manufactured by CNC milling machining and the vias have been metalized by using conductive paste (Fig. 2*b*). The Anritsu Universal Test Fixtures (UTF) 3680 and the Anritsu 37347C vector network analyzer (VNA) have been used for the measurements, and the comparison between HFSS simulations and measurements is shown in Fig. 2*c*. The experimental results confirm the large frequency separation between fundamental mode and second mode, which resonate at 4 GHz and 9 GHz, respectively.

III. Doublets with Side Coupling

The first coupling mechanism investigated in this work is the side coupling. It is obtained starting from the structure of Fig. 3*a*, consisting of two uncoupled quarter-mode resonators

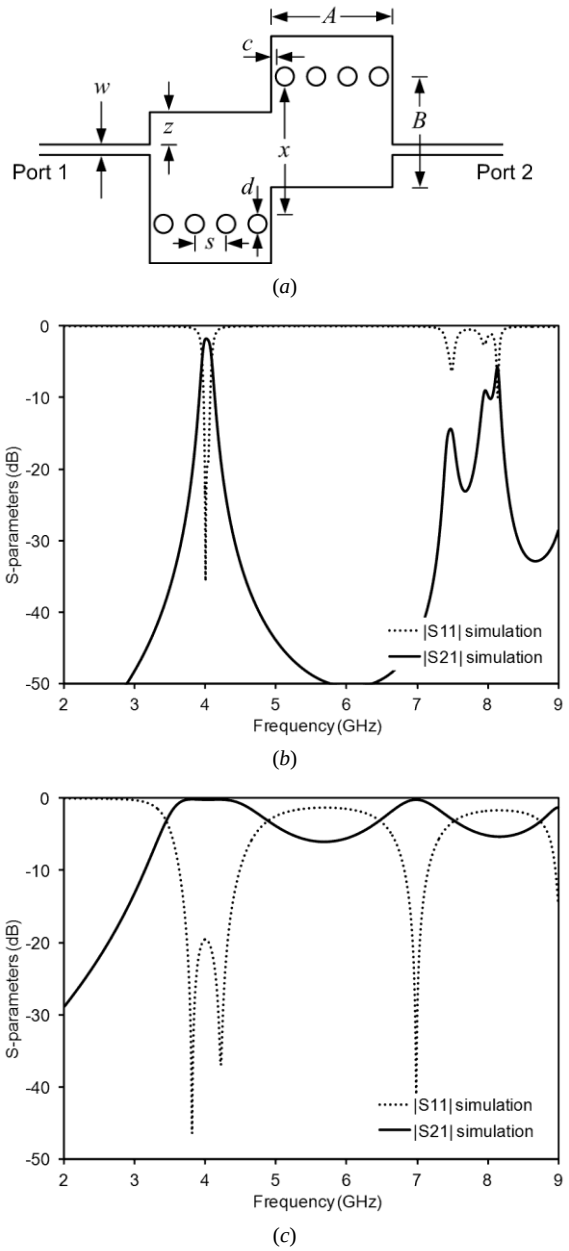

Fig. 4. Investigation of the lateral shift in quarter-mode SIW filter with side coupling: (*a*) geometry of the filter; (*b*) frequency response of a narrow band filter (dimensions in mm: *A*=14.0; *B*=13.0, *x*=6.5, *z*=9.5, *d*=2.0, *s*=3.66, *w*=1.2, *c*=0.5); (*c*) frequency response of a wide band filter (dimensions in mm: *A*=14.0; *B*=13.0, *x*=14.3, *z*=0, *d*=2.0, *s*=3.66, *w*=1.2, *c*=0.5).

sharing a post wall, and then removing some posts to create an aperture, as shown in Fig. 3*b*.

Two possible techniques are here considered to modify the coupling between resonators in side-coupled quarter-mode SIW cavities. The first technique, illustrated in Fig. 4*a* shows a doublet with side coupled resonators, where the desired coupling is achieved by laterally shifting the resonators of a quantity *x*, thus resulting in a change of the aperture size. In addition, the desired coupling between resonator and microstrip feeding line is obtained by shifting the microstrip line along the open side of the resonator, from the point with maximum electric field (*z*=0) to the one where the electric field vanishes (*z*=*B*).

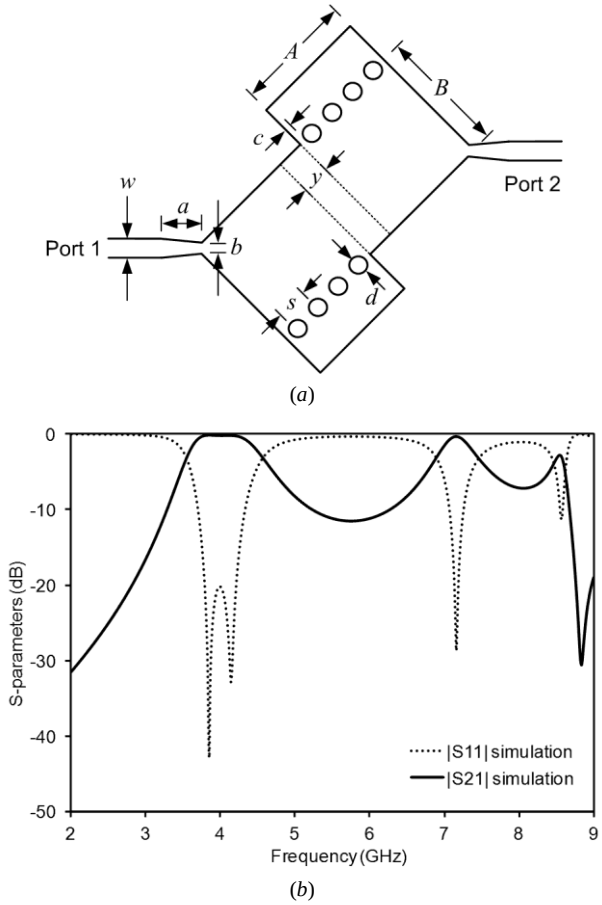

Fig. 5. Investigation of the cavity separation in quarter-mode SIW filter with side coupling (dimensions in mm: A=12.9, B=13.7, y=2.7, a=4.5, b=0.6, s=3.3, d=2.0, w=1.2): (*a*) geometry of the filter; (*b*) frequency response of the filter.

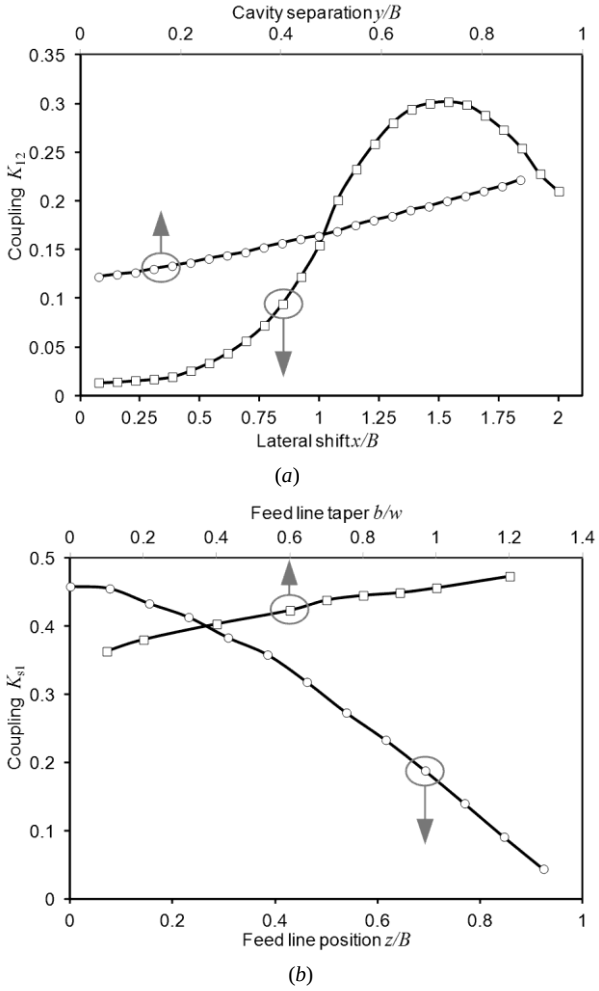

Fig. 6. Coupling coefficient in quarter-mode SIW cavities with side coupling: (*a*) internal coupling versus lateral shift and cavity separation; (*b*) external coupling versus feed line taper and position.

Two second-order band-pass filters centered at the frequency of 4 GHz have been designed by using this coupling topology: a narrow-band filter with fractional bandwidth FBW=1.7% is shown in Fig. 4*b* and a wide-band filter with FBW=17% is shown in Fig. 4*c*, thus demonstrating the high flexibility of the structure in terms of pass-band. In both cases, the substrate has a thickness of 0.508 mm, dielectric permittivity ε_r=3.5 and loss tangent tanδ=0.0018.

The second technique to control the side coupling is shown in Fig. 5*a*. In this case, the desired coupling is obtained by modifying the spacing y between the cavities. Moreover, Fig. 5*a* also shows a different technique for the control of the coupling between resonator and feeding line: instead of shifting the microstrip line along the open side of the resonator, a taper is adopted in this case, being the line connected to the point with maximum electric field. A filter based on this doublet configuration was designed to show the effectiveness of the proposed topology: Fig. 5*b* shows the frequency response of the filter. The same substrate of the previous examples was adopted.

The main difference between the structure of Fig.4*a* and the one of Fig. 5*a* is related to the achievable bandwidth: the first one allows designing filters with bandwidth ranging from narrow to wide, whereas with the second one the achievable bandwidth variation is more limited. This feature is related to the range of variation of the coupling coefficients. The doublet with lateral shift in Fig. 4*a* is able to cover wider coupling ranges, both for the case of coupling between resonators and coupling between resonator and feeding line. Fig. 6*a* shows the variation of the coupling coefficient between resonators in the case of lateral shift versus the amount of shift x normalized to the cavity size B (lower horizontal axis). The coupling is practically null for x=0: in this case, the structure can be seen as a waveguide, where the side wall boundary condition is electric wall on one side and magnetic wall on the other side. The left part and the right part of the structure exhibit opposite side wall condition, and for this reason the coupling is low. When x=2 B, the two resonators are physically separated, and the coupling suddenly drops to zero. The maximum appears around x=1.5 B, where the opposite side walls are far enough, but the two resonators share a large portion of the open side. As a comparison, Fig. 6*a* also shows the variation of the coupling coefficient between resonators in the case of cavity separation versus the distance y/B (upper horizontal axis): it is evident how the possibility to control the coupling coefficient is limited in this case.

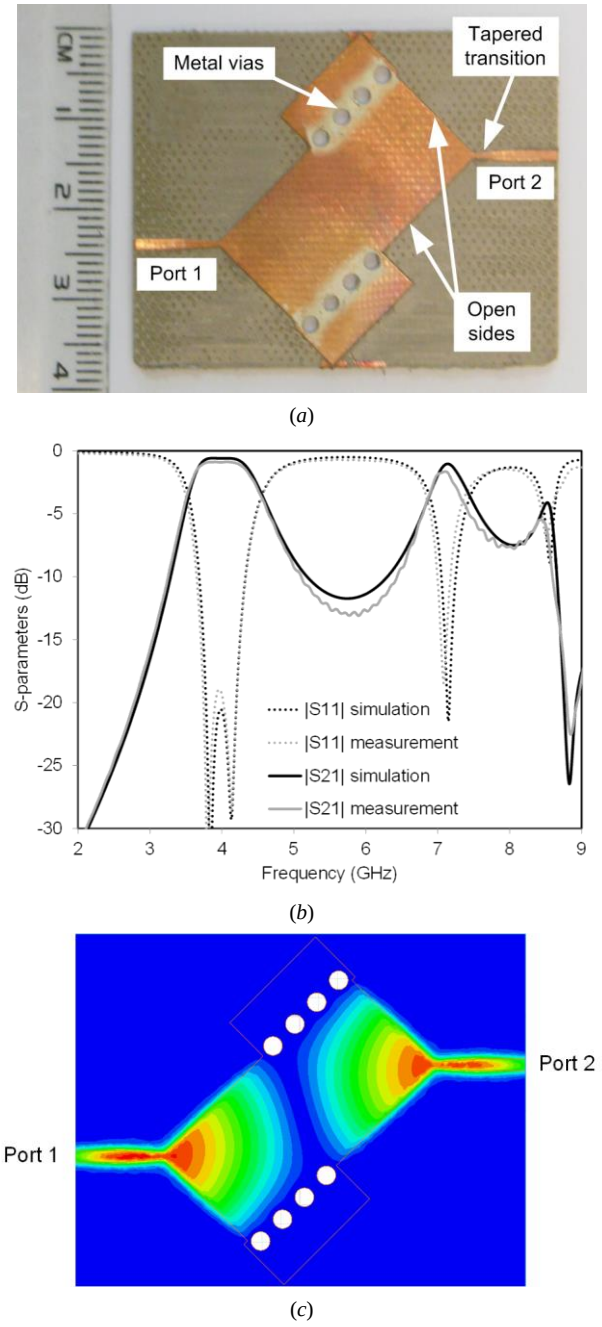

Fig. 7. Side-coupled two-pole filter in quarter-mode SIW technology (dimensions in the caption of Fig. 5): (*a*) photograph of the prototype; (*b*) simulated and measured scattering parameters; (*c*) plot of the amplitude of the electric field at the frequency of 4 GHz.

Coupling coefficients of Fig. 6*a* are calculated from the first two resonances (f_1 and f_2) of the structure composed by the two coupled resonators by using the formula [21] [22]:

$$|K| = \frac{\left|f_2^2 - f_1^2\right|}{f_2^2 + f_1^2}$$

Similarly, Fig. 6*b* shows the coupling between the resonator and the input microstrip line, versus the lateral shift *z* normalized to the cavity size *B*, in the case of Fig. 4*a* (lower horizontal axis), and versus the feed line taper *b* normalized to the line width *w*, in the case of Fig. 5*a* (upper horizontal axis).

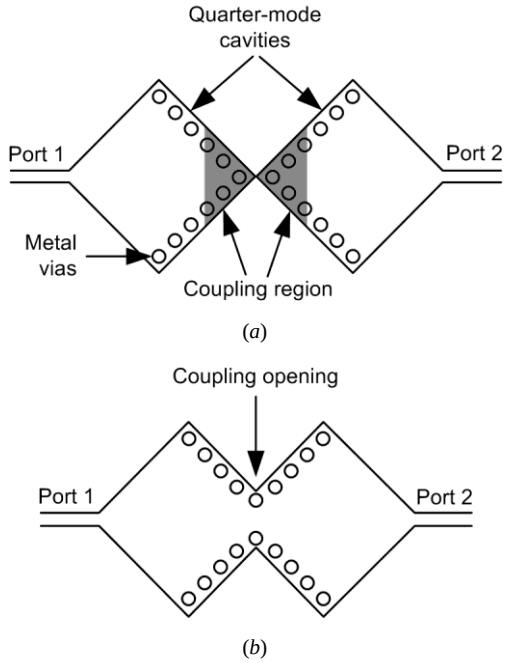

Fig. 8. Quarter-mode SIW filter with corner coupling: (*a*) two separated quarter-mode SIW cavities (the dark gray area denotes the coupling region); (*b*) schematic of the two-cavity filter with corner coupling.

Couplings to feeding lines have been here extracted from full-wave responses by exploiting the equivalent circuit. In the case of Fig. 4*a*, the coupling is maximized if the feed line is connected to the point with the most intense electric field (z=0) and minimized when it is shifted towards the metal vias (z=B). Conversely, when using the taper in Fig. 5*a*, the variation of the coupling is more limited. The results of Fig. 6 can also be used to design filter of various order. Of course all parameters can also be used at the same time, resulting in a structure where the coupling coefficient between feeding line and resonator is determined by the value of *z* and *b* while the coupling between resonators is determined by *x* and *y*.

A filter centered at 4 GHz with FBW=12% was manufactured to experimentally verify the results presented in this section. Fig. 7*a* shows the photo of the manufactured prototype, which is based on the design of Fig. 5. As in the case of the quarter SIW cavity, the structure was fabricated by CNC milling machining and the posts are filled with conductive paste. In Fig. 7*b*, the measured scattering parameters are compared with simulations, showing a good agreement both for the in-band and out-of-band frequency response, as well as for the transmission loss: the simulated transmission loss is 0.60 dB while the measured one is 0.91 dB. To clearly show the quarter-mode nature of this structure, the amplitude of the electric field at the central frequency of 4 GHz is illustrated in Fig. 7*c*, showing the maximum intensity in the corner of the cavity, near the feed point.

The footprint of this filter is 28.53x36.88 mm^2. In order to carry out a comparison between different circuits, the footprint of the device is intended without feeding lines and transitions, and it only concerns the area of the resonant cavities.

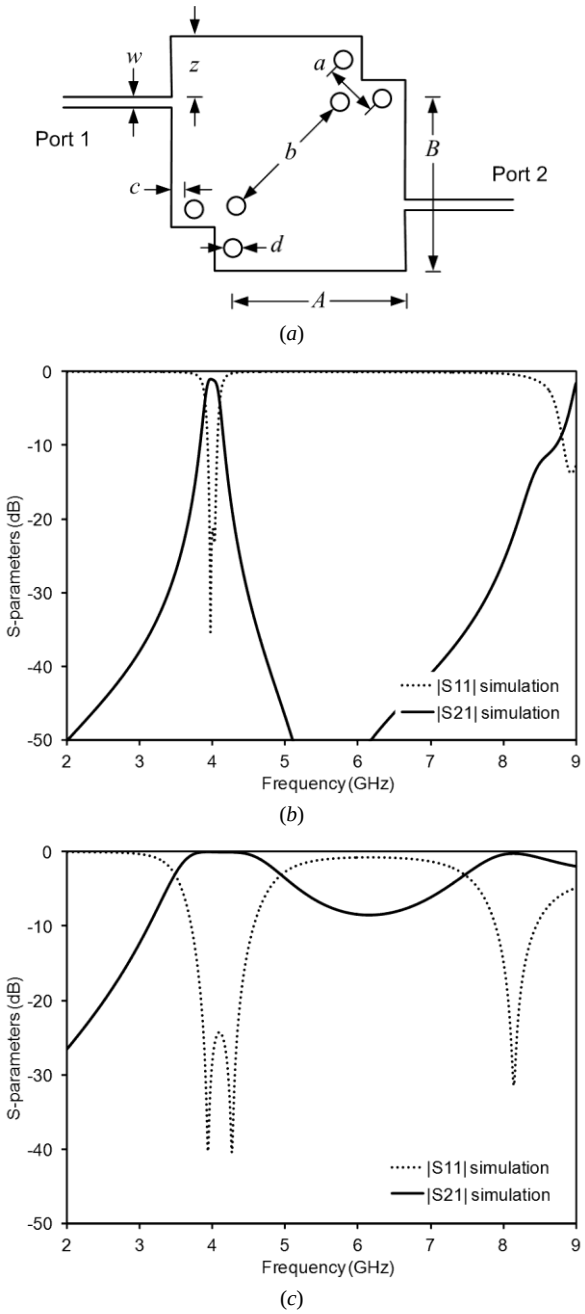

Fig. 9. Investigation of the quarter-mode SIW filter with corner coupling: (*a*) geometry of the filter; (*b*) frequency response of a narrow band filter (dimensions in mm: *A*=15.5, *B*=15.5, *z*=10.43, *a*=5.46, *b*=7.8, *d*=2, *w*=1.2, *c*=0.5); (*c*) frequency response of a wide band filter (dimensions in mm: *A*=14, *B*=14, *z*=0, *a*=5.46, *b*=17, *d*=2, *w*=1.2, *c*=0.5).

IV. Doublets with Corner Coupling

Another possible mechanism to couple quarter-mode SIW resonators is through their corners. As shown in Fig. 8, the idea is to remove the corner posts and then to partially overlap the two resonators, thus creating an aperture connecting them (Fig. 8*b*). In the proximity of the corner the electromagnetic field is weak and the corner removal produces a negligible change in resonant frequency, while the overlapping allows for more compact structures (the area can be reduced up to approximately 40%). Increasing the overlap allows for larger apertures, which result in wider band filters. Furthermore, the higher the overlapping the smaller the structure footprint.

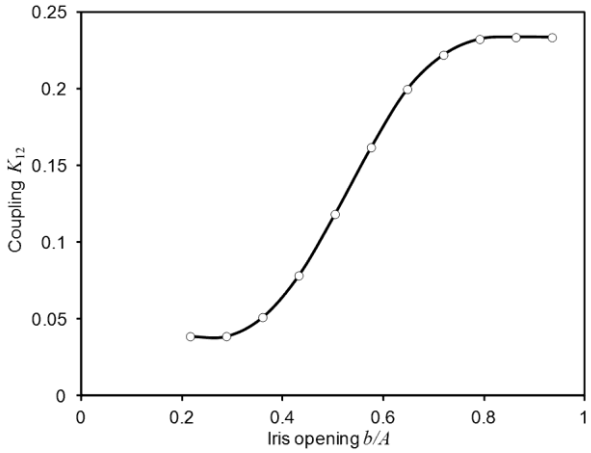

Fig. 10. Coupling coefficient in quarter-mode SIW cavities with corner coupling: internal coupling versus aperture of the iris window.

Once the distance between the two cavities has been fixed (determining the overlap area and the maximum aperture size), the coupling in corner-coupled quarter-mode SIW cavities can be changed by varying the distance *b* between the two central post, which determines the actual aperture size (Fig. 9*a*). In this structure, input and output couplings are controlled by shifting the feeding lines (as in the structure of Fig. 4*a*). The response of a narrow-band band-pass filter (FBW = 2.6%) and a wide-band band-pass filter (FBW = 16%) based on this circuit topology are shown in Figs. 9*b* and 9*c*, respectively, thus demonstrating the high flexibility of this structure in term of pass-band width.

Fig. 10 shows the coupling between resonators as a function of the distance *b* between central posts, normalized to the cavity size *B*. The maximum achievable coupling is slightly smaller than the one obtained by the structure of Fig. 4*a* and shown in Fig. 6*a*. Concerning the coupling between resonator and feeding line, the coupling mechanism is identical to the one adopted in the previous example, whose results are shown in Fig. 6*b*. This is the reason why the maximum achievable pass-band is similar in the two structures. In fact, in both structures the bottleneck limiting the bandwidth is represented by the maximum achievable coupling between resonator and feeding line.

Finally, a two-pole filter prototype based on corner-coupled quarter-mode cavities has been designed and manufactured. The center frequency is 4 GHz and the FBW is 13%. The structure of the filter and a photograph of the prototype are shown in Fig. 11*a* and Fig. 11*b*, respectively. The simulated and measured frequency responses are compared in Fig. 11*c*, showing a very good agreement both in the in-band and out-of-band regions. The measured insertion loss at 4 GHz is 0.8 dB. This filter topology leads to a size reduction compared with the previous structure, with a footprint of 26.59x24.79 mm^2.

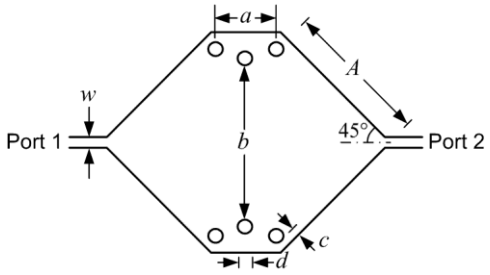

(*a*)

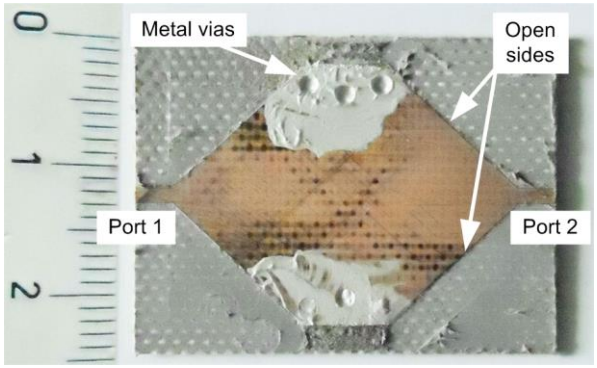

(*b*)

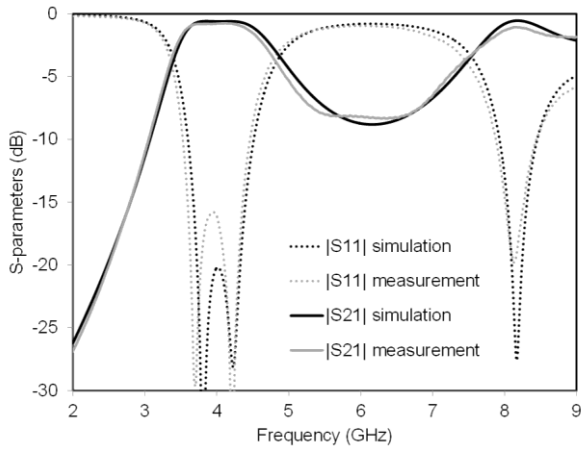

(*c*)

Fig. 11. Corner-coupled two-pole filter in quarter-mode SIW technology (dimensions in mm: A=13.9, a=5.6, b=14.4, s=2.9, d=1.5, w=1.2): (*a*) drawing of the structure; (*b*) photograph of the prototype; (*c*) simulated and measured scattering parameters.

V. Higher-Order Quarter Mode SIW Filters

A simple way to obtain N-th order quarter-mode SIW filters consists in cascading N side-coupled resonators, as shown in Fig. 12, where the case of a fourth-order filter is considered. In particular, the filter scheme with relevant parameters is shown in Fig. 12*a*, while the photograph of the prototype is shown in Fig. 12*b* (before the metallization of the posts). Note that, on the contrary of the geometry proposed in [10] and [11], this configuration allows filters of any order. To better recognize each cavity, some white circles have been added to the photo to indicate the layout of the quarter-mode cavities before removing some posts for proper coupling.

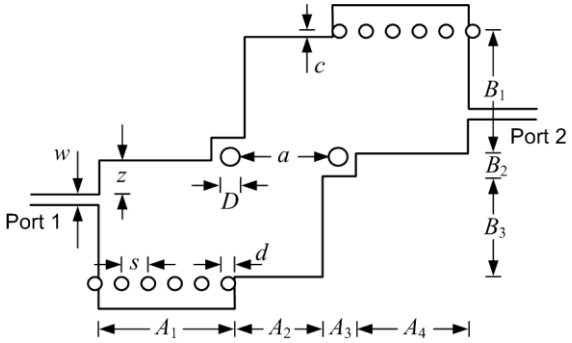

(*a*)

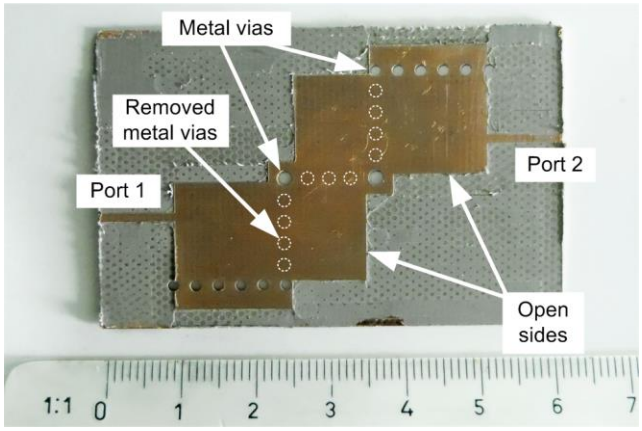

(*b*)

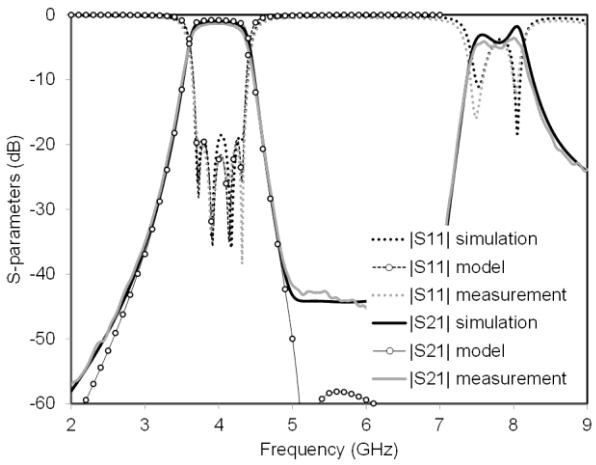

(*c*)

Fig. 12. Side-coupled four-pole filter in quarter-mode SIW technology (dimensions in mm: A_1=15.7, A_2=9.9, A_3=3.6, A_4=12.5, B_1=13.85, B_2=2.65, B_3=11.5, a=10.1, c=0.5, z=3.6, D=2, s=3, d=1.5, w=1.2): (*a*) drawing of the structure; (*b*) photograph of the prototype; (*c*) simulated and measured scattering parameters.

The four-pole filter was designed at 4 GHz and with FBW of 16%. In Fig. 12*c* simulation and measurement are plotted, showing a very good agreement. The measured insertion loss is 1.37 dB at the frequency of 4 GHz. This leads to a measured quality factor Q=90. The topology of the filter is shown in Fig. 13*a*, and the corresponding coupling matrix is reported in Fig. 13*b*. Note that also coupling between resonators 1 and 3 (as well as between 2 and 4) have been taken into account.

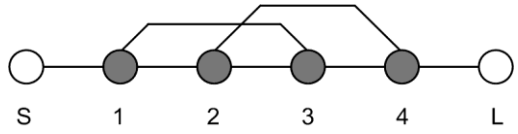

(*a*)

	S	1	2	3	4	L
S	0	1.0216	0	0	0	0
1	1.0216	0.0062–*j* 0.0414	0.8843	0.0985	0	0
2	0	0.8843	–0.1231–*j* 0.0414	0.6892	0.0985	0
3	0	0.0985	0.6892	–0.1231–*j* 0.0414	0.8843	0
4	0	0	0.0985	0.8843	0.0062–*j* 0.0414	1.0216
L	0	0	0	0	1.0216	0

(*b*)

Fig. 13. Equivalent circuit model of the side-coupled four-pole filter in quarter-mode SIW technology: (*a*) filter topology; (*b*) coupling matrix.

Those additional couplings are due to the direct connection between resonators 1 and 3 (2 and 4) due to the field coupling outside the aperture *a* in Fig. 12*a*. These additional couplings allow for transmission zeros. Actually, the first version of the filter has been designed without taking into account the cross-couplings. Cross-couplings have then been added to the first filter version by increasing the values of A_3 and B_2 (Fig. 12*a*). This change slightly modified the in-band behavior, requiring a small re-optimization of the filter. Cross-coupling values have been finally extracted from the full-wave response. The coupling matrix in Fig. 13*b* has been computed by considering a quality factor Q=151, derived in Sec. II, Table I. The frequency response obtained from the coupling matrix is also reported in Fig. 12*c*. Coupling matrix parameters represent the normalized version of the coupling coefficients in Fig. 6 and Fig. 10 in terms of fractional bandwidth [21][22].

Quarter-mode cavities can be also combined in a different fashion, including the mixture with different resonators. Fig. 14 shows an example, where a coplanar resonator is used together with a pair of corner-coupled quarter-mode cavities, to obtain a three-pole filter. The geometry of the filter is shown in Fig. 14*a*, while the photograph of the prototype is reported in Fig. 14*b*. The coplanar resonator consists of two identical slots, symmetrically placed at the top of the SIW. A three-pole filter was designed, centered at 4 GHz with FBW=16%. The simulated and measured frequency response is shown in Fig. 14*c*. The measured insertion loss is 1.02 dB at 4 GHz. The footprint of the resulting manufactured filter is 31.39x22.06 mm^2, larger than the two-pole filter shown in Fig. 11. This size increase is due to the fact that the two cavities are placed at higher distance to obtain enough room for housing the coplanar resonator. However, a reduction of about 30% with respect to the prototype of Fig. 7 is obtained and this is a good result, especially considering that this is a 3-pole filter.

The topology of the three-pole filter is shown in Fig. 15*a*, where resonators 1 and 3 (representing the two quarter mode cavities) are connected through the aperture obtained removing the corner posts and through the resonator 2(representing the coplanar). This topology allows for a transmission zero that, according to the sign of the coupling, is

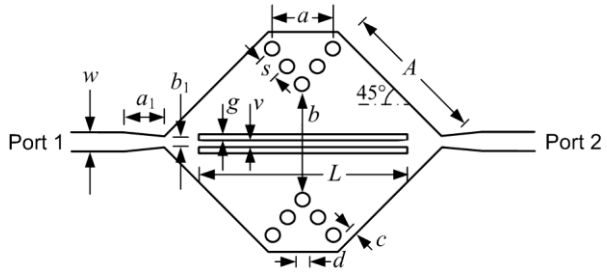

(*a*)

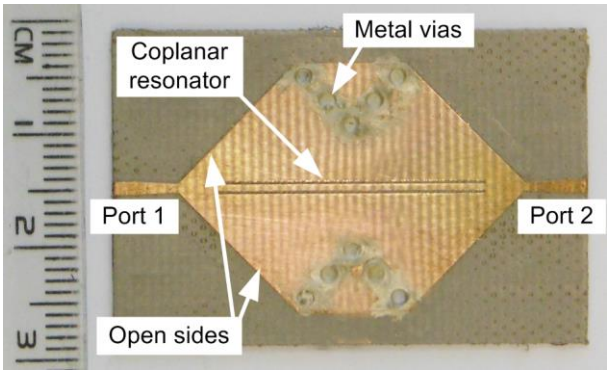

(*b*)

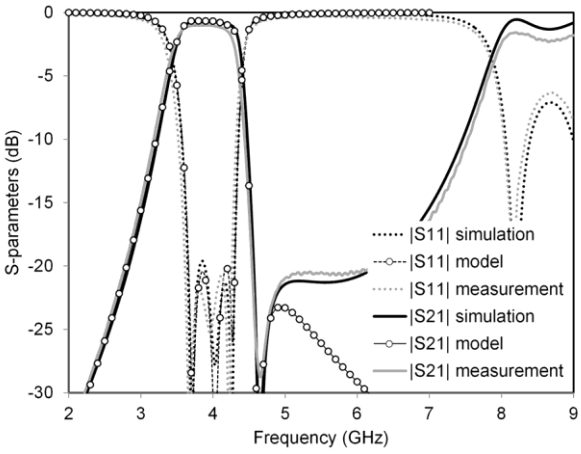

(*c*)

Fig. 14. Corner-coupled three-pole filter in quarter-mode SIW technology with additional coplanar resonator (dimensions in mm: A=15.6, a=8.5, b=9.7, a_1=3.87, b_1=0.74, L=24.1, g=0.25, v=0.6, s=2.1, d=1.5, w=1.2): (*a*) drawing of the structure; (*b*) photograph of the prototype; (*c*) simulated and measured scattering parameters.

place in the upper stop-band. This zero can be placed very close to the filter band resulting in a high selectivity in the upper cutoff of the filter band. Similarly to the previous structure, the coupling matrix in Fig. 15*b* has been computed by considering a quality factor Q=151. The frequency response obtained from the coupling matrix is shown in Fig. 14*c*.

In this case, unlike the structure of Fig. 9*a*, the input coupling mechanism is the same as in Fig. 7, where tapered feeding lines are connected to the open corner of the quarter mode resonators. This feeding mechanism preserves the symmetry of the structure, avoiding the undesired coupling of spurious coplanar modes. The desired coupling between the quarter mode cavities and the coplanar resonator is obtained

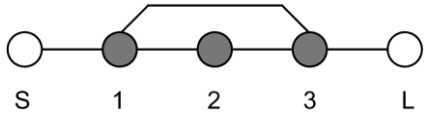

(*a*)

	S	1	2	3	L
S	0	1.0715	0	0	0
1	1.0715	0.2316–*j* 0.0401	0.8789	0.5894	0
2	0	0.8789	–0.4754–*j* 0.0401	0.8789	0
3	0	0.5894	0.8789	0.2316–*j* 0.0401	1.0715
L	0	0	0	1.0715	0

(*b*)

Fig. 15. Equivalent circuit model of the corner-coupled three-pole filter in quarter-mode SIW technology: (*a*) filter topology; (*b*) coupling matrix.

by properly selecting the distance between the slots and/or the slot width. The transmission zeros are mainly controlled by the coupling between the two quarter-mode resonators. Conversely, the resonance frequency of the coplanar line depends on the slot length. According to the coupling matrix of Fig. 15*b*, the resonance frequency of the coplanar resonator is higher than that of the quarter-mode cavities.

VI. Conclusion

This paper has presented a systematic investigation of SIW filters based on quarter-mode cavity resonators. This class of filters exhibit reduced size compared to classical SIW cavity filters, while preserving most of the advantages of SIW structures. A comparison of the different SIW filter topologies is reported in Table II.

Some new configurations and topologies have been proposed, and different coupling mechanisms between quarter-mode cavities and between input line and cavity have been described. The feasibility of the proposed approaches is demonstrated through several designs and manufactured prototypes.

These filters demonstrate a large design flexibility, compact size, possibility of introducing transmission zeros, as well as the option to combine SIW cavities with coplanar-line resonators. They represent a valuable solution when the size of the SIW is an issue, especially at relatively low operation frequency.

TABLE II Comparison of filters with different SIW cavities.

	Cavity size	Advantages	Disadvantages
Standard cavity	λ/2×λ/2	Complete shielding	Relatively large size
Half-mode cavity	λ/4×λ/2	Compact size	One open side (radiation)
Quarter-mode cavity	λ/4×λ/4	Very compact, Flexible topology	Two open sides (radiation)

References

[1] M. Bozzi, A. Georgiadis, and K. Wu, "Review of Substrate Integrated Waveguide (SIW) Circuits and Antennas," *IET Microwaves, Antennas and Propagation*, Vol. 5, No. 8, pp. 909–920, June 2011.

[2] D. Deslandes and K. Wu, "Integrated microstrip and rectangular waveguide in planar form," *IEEE Microwave and Wireless Components Letters*, Vol. 11, No. 2, pp. 68-70, Feb. 2001.

[3] N. Grigoropoulos, B.S. Izquierdo, and P.R. Young, "Substrate Integrated Folded Waveguides (SIFW) and Filters," *IEEE Microwave and Wireless Components Letters*, Vol. 15, No. 12, pp. 829-831, Dec. 2005.

[4] W. Hong *et al*., "Half Mode Substrate Integrated Waveguide: A New Guided Wave Structure for Microwave and Millimeter Wave Application," *Proc. Joint 31st Intern. Conf. Infrared Millimeter Waves and 14th Intern. Conf. Terahertz Electronics*, p. 219, Shanghai, China, Sept. 18–22, 2006.

[5] X. Chen and K. Wu, "Substrate Integrated Waveguide Filter: Basic Design Rules and Fundamental Structure Features," *IEEE Microwave Mag*., Vol. 15, No. 5, pp. 108–116, Jul./Aug. 2014.

[6] T. Yang, P.-L. Chi, R. Xu, and W. Lin, "Folded Substrate Integrated Waveguide Based Composite Right/Left-Handed Transmission Line and Its Application to Partial H -Plane Filters," *IEEE Trans. Microwave Theory Techn.*, Vol. 61, No. 2, pp. 789-799, Feb. 2013.

[7] R. Moro, S. Moscato, M. Bozzi, and L. Perregrini, "Substrate Integrated Folded Waveguide Filter with Out-of-Band Rejection Controlled by Resonant-Mode Suppression," *IEEE Microwave and Wireless Components Letters*, Vol. 25, No. 4, pp. 214-216, April 2015.

[8] Y. Wang *et al.*, "Half Mode Substrate Integrated Waveguide (HMSIW) Bandpass Filter," *IEEE Microwave and Wireless Components Letters*, Vol. 17, No. 4, pp. 265–267, April 2007.

[9] M. Rezaee and A.R. Attari, "Realisation of new single-layer triple-mode substrate integrated waveguide and dual-mode half-mode substrate-integrated waveguide filters using a circular shape perturbation," *IET Microwaves, Antennas & Propagation*, Vol. 7, No. 14, pp. 1120-1127, Nov. 2013.

[10] Z. Zhang, N. Yang, and K. Wu, "5-GHz bandpass filter demonstration using quarter-mode substrate integrated waveguide cavity for wireless systems," *IEEE Radio and Wireless Symposium 2009*, pp. 95-98, San Diego, CA, USA, 18-22 Jan. 2009.

[11] K. Deng, Z.X. Guo, W. Che, Q. Xue, "A compact bandpass filter using quarter SIW cavity resonator with source-load cross coupling," *2011 41st European Microwave Conference*, pp. 732-735, Manchester, UK, 10-13 Oct. 2011.

[12] Y. Jiang *et al*., "A reconfigurable filter based on quarter-mode substrate integrated waveguide (QMSIW) resonator," *2013 Cross Strait Quad-Regional Radio Science and Wireless Technology Conference*, pp. 5-7, Chengdu, China, 21-25 July 2013.

[13] M.Z. Ur Rehman *et al*., "Microwave bandpass filter using QMSIW," *2013 IEEE International RF and Microwave Conference*, pp.172-175, Penang, Malaysia, 9-11 Dec. 2013.

[14] D.E. Senior, A. Rahimi, and Y.-K. Yoon, "A surface micromachined broadband millimeter-wave filter using quarter-mode substrate integrated waveguide loaded with complementary split ring resonator," *2014 IEEE MTT-S International Microwave Symposium*, pp. 1-4, Tampa, FL, USA, 1-6 June 2014.

[15] C. Jin and Z. Shen, "Compact Triple-Mode Filter Based on Quarter-Mode Substrate Integrated Waveguide," *IEEE Trans. Microwave Theory Techn*., Vol. 62, No. 1, pp. 37-45, Jan. 2014.

[16] X. Zhang, C. Ma, and F. Wang, "Design of compact dual-passband LTCC filter exploiting stacked QMSIW and EMSIW," *Electronics Letters*, Vol. 51, No. 12, pp. 912-914, Nov. 2015.

[17] A.P. Saghati, A.P. Saghati, and K. Entesari, "An ultra-miniature quarter-mode SIW bandpass filter operating at first negative order resonance," *2015 IEEE MTT-S Intern. Microwave Symposium*, pp.1-3, Phoenix, AZ, USA, 17-22 May 2015.

[18] Y.M. Huang, Z. Shao, C.J. You, and G.Wang, "Size-reduced bandpass filters using quarter-mode substrate integrated waveguide loaded with different defected ground structure patterns," *2015 IEEE MTT-S Intern. Microwave Symposium*, pp.1-4, Phoenix, AZ, USA, 17-22 May 2015.

[19] A.P. Saghati, S.B. Kordmahale, J. Kameoka, and K. Entesari, "A reconfigurable quarter-mode substrate integrated waveguide cavity filter employing liquid-metal capacitive loading," *2015 IEEE MTT-S Intern. Microwave Symposium*, pp.1-3, Phoenix, AZ, USA, 17-22 May 2015.

[20] R.E. Collin, *Foundations for Microwave Engineering*, McGraw-Hill, Inc., New York, 1966.

[21] C. Tomassoni and R. Sorrentino, "A new class of pseudoelliptic waveguide filters using dual-post resonators," *IEEE Trans. Microwave Theory Techn.*, Vol. 61, No. 6, pp. 2332-2339, June 2013.

[22] C. Tomassoni, S. Bastioli, and R.V. Snyder, "Propagating Waveguide Filters Using Dielectric Resonators," *IEEE Trans. Microwave Theory Techn.*, Vol. 63, No. 12, pp. 4366–4375, Dec. 2015.

Stefano Moscato (S'12) received the M.S. and Ph.D. degrees in electronic engineering from the University of Pavia, Pavia, Italy, in 2012 and 2016, respectively. From December 2014 to April 2015, he was with the School of Electrical and Computer Engineering, Georgia Institute of Technology, Atlanta, GA, USA, as a Ph.D. visiting student. He is currently with Azcom Technology, Rozzano (MI), Italy as RF designer for LTE and 5G base stations and remote radio heads. His research activities have focused on the implementation of RF and microwave passive components in substrate-integrated waveguide (SIW) technology based on standard substrates, ecofriendly materials and by exploiting the innovative 3D printing technique. Dr. Moscato has been the chair of the IEEE Student Branch, University of Pavia, since 2013. He was the recipient of an IEEE Microwave Theory and Techniques Society (IEEE MTT-S) Undergraduate/Pre-Graduate Scholarship in 2012.

Cristiano Tomassoni (M'15) was born in Spoleto, Italy. He received the Laurea degree and Ph.D. degree in electronics engineering from the University of Perugia, Perugia, Italy, in 1996 and 1999, respectively. His dissertation concerned the mode-matching analysis of discontinuities involving elliptical waveguides. In 1999, he was a Visiting Scientist with the Lehrstuhl für Hochfrequenztechnik, Technical University of Munich, Munich, Germany, where he was involved with the modeling of waveguide structures and devices by using the generalized scattering matrix (GSM) technique. From 2000–2007, he was a Postdoctoral Research Associate with the University of Perugia. In 2001, he was a Guest Professor with the Fakultät für Elektrotechnik und Informationstechnik, Otto-von-Guericke University, Magdeburg, Germany. During that time, he was involved with the modeling of horn antennas having nonseparable cross sections by using hybrid methods combining three different techniques: the finite-element method, mode-matching technique, and generalized multipole technique. He was also involved in the modeling of low-temperature co-fired ceramics by using the method of moments. He studied new analytical methods to implement boundary conditions in the transmission-line matrix method, and he modeled aperture antennas covered by dielectric radome by using spherical waves. Since 2007, he has been an Assistant Professor with the University of Perugia. His main area of research concerns the modeling and design of waveguide devices and antennas. His research interests also include the development of reduced-size cavity filters, reconfigurable filters, and printed reconfigurable antenna arrays. Dr. Tomassoni was the recipient of the 2012 Microwave Prize presented by the IEEE Microwave Theory and Technique Society.

Maurizio Bozzi (S'98–M'01–SM'12) was born in Voghera, Italy, in 1971. He received the Ph.D. degree in electronics and computer science from the University of Pavia, Pavia, Italy, in 2000.

He held research positions with various universities worldwide, including the Technische Universität Darmstadt, Darmstadt, Germany; the Universitat de Valencia, Valencia, Spain; and the École Polytechnique de Montréal, Montreal, QC, Canada. In 2002, he joined the Department of Electronics, University of Pavia, where he is currently an Associate Professor. He has authored or co-authored more than 90 journal papers and 240 conference papers. He co-edited the book Periodic Structures (Research Signpost, 2006) and co-authored the book Microstrip Lines and Slotlines (Artech House, 2013).

His main research interests concern the computational electromagnetics, the substrate integrated waveguide technology, and the use of novel materials and fabrication technologies for microwave circuits (including paper, textile, and 3D printing).

Prof. Bozzi is the 2016 Secretary of the IEEE Microwave Theory and Techniques Society (MTT-S) and a member of the General Assembly (GA) of the European Microwave Association (EuMA) for the 2014–2016 term. He is an associate editor for the IEEE MICROWAVE AND WIRELESS COMPONENTS LETTERS, the IET Electronics Letters, and the IET Microwaves, Antennas and Propagation. He was the General Conference Chair of the IEEE International Conference on Numerical Electromagnetic Modeling and Optimization, NEMO2014, Pavia, Italy, 2014, and the General Chair of the IEEE MTT-S International Microwave Workshop Series on Millimeter Wave Integration Technologies, Sitges, Spain, 2011.

He received several awards, including the 2015 Premium Award for Best Paper in IET Microwaves, Antennas & Propagation, the 2014 Premium Award for the Best Paper in Electronics Letters, the Best Young Scientist Paper Award of the XXVII General Assembly, URSI, in 2002, and the MECSA Prize of the Italian Conference on Electromagnetics (XIII RiNEm), in 2000.

Luca Perregrini (M'97–SM'12–F'16) received the Laurea degree in electronic engineering and Ph.D. degree in electronics and computer science from the University of Pavia, Pavia, Italy, in 1989 and 1993, respectively. In 1992, he joined the Department of Electronics of the University of Pavia, Pavia, Italy, where he is now an Associate Professor of electromagnetics. He was an Invited Professor at the Polytechnic University of Montreal, Montreal, QC, Canada, in 2001, 2002, 2005, and 2006.

His main research interests are in numerical methods for the analysis and optimization of waveguide circuits, frequency-selective surfaces, reflectarrays, printed microwave circuits, substrate integrated circuits, large reflector antennas, and industrial application of microwaves.

Prof. Perregrini is the Editor in Chief of the IEEE TRANSACTIONS ON MICROWAVE THEORY AND TECHNIQUES for the term 2017-2019, and an associate editor of the International Journal of Microwave and Wireless Technologies, and an associate editor of the IET Electronic Letters. He is a member of the Board of Directors of the European Microwave Association for the term 2016-18. He was the Technical Program Chair of the European Microwave Conference (EuMC 2014) and of the IEEE International Conference on Numerical and Electromagnetic Modeling and Optimization (NEMO2014), a member of the Technical Program Review Committee of the IEEE International Microwave Symposium (since 2003) and of the Technical Program Committee of the European Microwave Conference (since 2009). He has been an associate editor of the IEEE MICROWAVE AND WIRELESS COMPONENTS LETTERS (2010–13) and of the IEEE TRANSACTIONS ON MICROWAVE THEORY AND TECHNIQUES (2013-2016), and a member of the General Assembly of the European Microwave Association (2011–13). He has authored or co-authored more than 80 papers published in international journals, more than 230 conference papers, six book chapters, a textbook on electromagnetic waves, and an exercise book on electric circuits. He was the co-editor of the book Periodic Structures (Research Signpost, 2006).